Asymptotic analysis of radio frequency heated collisional plasma

Nathaniel J. Fisch and Charles F. F. Karney

Citation: Physics of Fluids (1958-1988) **28**, 3107 (1985); doi: 10.1063/1.865352
View online: http://dx.doi.org/10.1063/1.865352
View Table of Contents: http://scitation.aip.org/content/aip/journal/pof1/28/10?ver=pdfcov
Published by the AIP Publishing

Asymptotic analysis of radio frequency heated collisional plasma

Nathaniel J. Fisch and Charles F. F. Karney
Princeton Plasma Physics Laboratory, Princeton, New Jersey 08544

(Received 25 February 1985; accepted 20 June 1985)

It is shown that a distribution of electrons in resonance with traveling waves, but colliding with background distributions of electrons and ions, evolves to a steady state. Previously, the existence of such solutions had been assumed, but not proved, in numerical and other calculations. Details of the steady state are given analytically in the asymptotic limit of high electron energy and are compared with numerical solutions. The asymptotic analytic solution may be useful for quickly relating emission data to likely excitations and is more reliable than conventional numerical solutions at high energy. A method of improving numerics at high energy is suggested.

I. INTRODUCTION

Quasilinear theory deals with the collisionless interaction of radio-frequency (rf) waves with a plasma and predicts the well-known flattening of the electron distribution function in the region of velocity space resonant with the waves. Fokker–Planck theory presents the competing effect of interparticle binary Coulomb collisions that tends to relax the electrons to a Maxwellian distribution. Both theories are among the most strongly held and widely corroborated models in theoretical plasma physics. In the presence of both rf waves and binary collisions, several interesting and useful phenomena occur, including plasma heating and current generation.

The theoretical treatment of the velocity space behavior of electrons undergoing these phenomena begins with the Fokker–Planck equation (see, e.g., Ref. 1) with an added diffusive term caused by the rf waves, namely,

$$\frac{\partial f}{\partial t} = C(f,f) + C(f,f_i) + \frac{\partial}{\partial \mathbf{v}} \cdot \mathsf{D} \cdot \frac{\partial}{\partial \mathbf{v}} f, \tag{1}$$

where $C(f,f)$ represents electrons with distribution f colliding with themselves, and $C(f,f_i)$ represents the electrons colliding with a given ion background. The self-collisions conserve energy and momentum, but in the limit of a large mass ratio, i.e., $m_i/m_e \gg 1$, the ion term exchanges momentum but not energy. For the purposes of investigating rf heating and current drive, $m_e/m_i \to 0$ is generally assumed in Eq. (1) and will be assumed here. The last term in Eq. (1) contains the effect of the waves, and we shall immediately specialize to the case where

$$\mathsf{D}(v) = \begin{cases} D_{\mathrm{QL}} \hat{i}_z \hat{i}_z, & v_1 < v_z < v_2, \\ 0, & \text{otherwise}, \end{cases} \tag{2}$$

with $\hat{i}_z$ the unit vector in the direction parallel to a constant magnetic field, D_{QL} a constant, and v_1, v_2 defining the limits of parallel phase velocities in the wave spectrum. Characterizing the rf spectrum in this way enables us to reduce the number of free parameters in the problem to just four: namely, $w_1 \equiv v_1/v_T$, $w_2 \equiv v_2/v_T$ where v_T is the electron thermal velocity; $D \equiv D_{\mathrm{QL}}/\nu_0 v_t^2$, where ν_0 is the collision frequency; and Z_i, the ion charge state. Equation (2) is suitable for describing the interaction of lower-hybrid waves with the plasma.

Although procedures have been developed[2] to facilitate solving the fully nonlinear equation (1), this is not necessary for our purposes and it remains far easier to solve the linearized equations. Even under strong rf excitation, f is nearly Maxwellian for most electrons so that we can expand

$$f = f_m + \hat{f}, \tag{3a}$$

$$C(f,f) \simeq C(\hat{f},f_m) + C(f_m,\hat{f}), \tag{3b}$$

where $\hat{f}$ represents the deviation of f from a Maxwellian f_m. In our notation, $C(\hat{f},f_m)$ represents the collisions of (test) distribution f with a Maxwellian background, and $C(f_m,\hat{f})$ represents the collisions of the Maxwellian background of the test distribution, viz., the self-consistent bulk heating by the test distribution. The term $C(\hat{f},\hat{f})$ is justifiably neglected even when $\hat{f}(\mathbf{v}) \gg f_m(v)$, which can occur on the tail of the distribution function. This is because tail electrons still collide far more with bulk electrons then with themselves. Note that the self-collision term for a Maxwellian distribution, i.e., $C(f_m,f_m)$, is zero.

Equation (1), with D given by Eq. (2), does not admit a steady-state solution, since rf waves put energy into electrons, but collisions offer no energy sink. This is true also when the linearized collision operator is used, since that operator, too, conserves energy. While a time-evolving distribution presents no conceptual difficulty, there are reasons for preferring to solve a slightly different equation, one that has a solution evolving to a steady state. Solving such an equation limits the parameter space of discussion to one less dimension. We expect, on a physical basis, that in any event some loss mechanisms will be present that serve to limit the bulk temperature and to achieve a steady state at some bulk temperature. It is then convenient to discuss heating rates, current generation efficiency, etc., as a function of this bulk temperature, rather than as a function of some initial temperature with time as a parameter.

To arrange a steady state, a dissipative term, i.e., a heat sink, must be introduced into Eq. (1), and the exact form of this sink will necessarily be *ad hoc*. A rather reasonable heat sink arises by assuming that some unspecified mechanism serves to keep the bulk of the electrons at some constant temperature, thereby negating the bulk heating effect of the collision term $C(f_m,\hat{f})$ in Eq. (3b). This allows us to approximate

$$C(f,f) \simeq C(f,f_m) \tag{3c}$$

 0031-9171/85/103107-09$01.90

in Eq. (1). The approximation (3c) is particularly good when the resonant electrons are fast, superthermal electrons, such as would occur in lower-hybrid heating and current generation.[3] For fast electrons, the detailed form of the bulk distribution is relatively unimportant, and, moreover, these electrons have little effect on the form of the bulk distribution other than to heat it. Approximation (3c) leaves only a Maxwellian background of scatterers, which serve also as a heat reservoir to bring the distribution to steady state.

Using Eqs. (2) and (3c), Eq. (1) has been solved numerically in previous work by the authors. Further arguments are advanced in Ref. 4 that discuss why these approximate equations describe current generation by lower-hybrid waves well. However, though tacitly assumed, it has not been proven that a steady-state solution does, in fact, exist. The reasoning above does not show that a heat sink is a sufficient condition for a steady state, only a necessary condition. For example, in the presence of a dc electric field, the electron distribution function exhibits runaways and no steady state, even with the heat sink provided by Eq. (3c). Neither do the numerical solutions of the Fokker–Planck equation prove the existence of a steady state, even though a numerical steady state is found. Rather, the numerical studies assume *a priori* the existence of such a state in the form of boundary conditions on the necessarily finite numerical mesh on which the computations are made.

In this paper we shall prove that Eqs. (1), (2), and (3c) reach a steady state. The proof consists of setting $\partial f/\partial t = 0$ in Eq. (1) and constructing an asymptotic (i.e., for $v \to \infty$) solution, which we show to be normalizable. Apart from academic interest (the numerical approach is neither general nor quick at exhibiting asymptotic behavior), such a proof is viewed as useful in that it justifies the numerical solution, indicating where the imposition of finite boundary conditions on a numerical grid is valid. Details of this solution might be checked experimentally by examining the radiation of very fast electrons.

Having obtained the asymptotic solution, we naturally wanted to try to use it to describe f analytically over all velocity space. Using a rather crude match to the Maxwellian region $u \to 0$, we were able to describe reasonably, if not rigorously, f and several important moments of it.

The paper is organized as follows. In Sec. II we set up the procedure for solving f analytically by matching fluxes at the boundaries of the resonant region. This procedure draws heavily on material presented in Ref. 5. In Sec. III we derive the asymptotic solution as $u \to \infty$. In Sec. IV we try to connect this solution to the Maxwellian region, to give a complete analytic description. In Sec. V we compare our analytic solution to a numerical integration. Section VI summarizes our findings.

II. STRONG-RF LIMIT

For fast electrons, Eqs. (1), (2), and (3c) can be cast in normalized form in spherical coordinates as

$$\frac{1}{\nu_0}\frac{\partial f}{\partial t} = \frac{\xi}{u^2}\frac{\partial}{\partial u}\left(\frac{1}{u}\frac{\partial f}{\partial u} + f\right) + \frac{1}{u^3}\frac{\partial}{\partial \mu}(1-\mu^2)\frac{\partial}{\partial \mu}f + \frac{\partial}{\partial w}D(w)\frac{\partial}{\partial w}f = 0\,, \tag{4a}$$

$$D(w) = \begin{cases} D\,, & w_1 < w < w_2\,, \\ 0\,, & \text{otherwise}\,, \end{cases} \tag{4b}$$

where velocities are normalized to the electron thermal speed, i.e., $u = v/v_{Te}$, $w = v_z/v_{Te}$; we use $\mu = w/u$ and define $\xi \equiv 2/(Z_i + 1)$; and we set Eq. (4a) to zero to find the steady state f. The limit of validity of this equation strictly includes only $u \gg 1$, but note that for $u < 1$ the solution tends, as it should, to a Maxwellian. [This large-u limit of the collision operator of Eq. (3c) has been used to predict analytically and with great accuracy the efficiency of current generation when $w_1 \gg 1$.[6]] While this gives us confidence in employing this limit, here we need the form of f, not merely the more easily calculated efficiency.

In the event that the rf diffusion is weak, i.e., $u^3 D \ll 1$, then Eqs. (4) are easily solved analytically by expanding f in Legendre harmonics of μ, exploiting the fact that coupling between the Legendre harmonics occurs only to higher order in D.[5] However, eventually, as $u \to \infty$, we obtain $u^3 D \gg 1$, indicating that asymptotically in u, the rf always flattens the distribution function in the resonant region. The weak-rf approach then breaks down and a strong-rf approach must be taken.

For the strong-rf limit, which is the proper limit for performing asymptotic, we divide velocity space into three regions: I, $w < w_1$; II $w_1 < w < w_2$; and III, $w > w_2$. In region II, where the resonant rf diffusion occurs, we can take D large and expand f in powers of $1/D$, i.e.,

$$f = f^{(0)} + (1/D) f^{(1)} + \cdots \tag{5}$$

and, to lowest order, Eq. (4) becomes

$$\frac{\partial^2}{\partial w^2} f^{(0)} = 0, \tag{6}$$

which has the solution

$$f^{(0)} = F(x) + wG(x), \tag{7}$$

where $x \equiv v_\perp / v_{Te}$ is the normalized perpendicular velocity. The functions F and G can be determined, however, only through matching to solutions in regions I and III. What must be matched at the boundaries $w = w_1$ and $w = w_2$ are the normal (i.e., w = directed) fluxes and f.

We can conclude immediately, however, that $G = 0$, since G contributes to the w-directed flux in region II to order D, which is so large that it cannot possibly be matched in regions I and III, where there is no rf, the fluxes can at most be order D^0. We shall, in general, be concerned only with the $D \to \infty$ limit and thus our solution in region II is simply

$$f = F(x), \quad w_1 < w < w_2. \tag{8}$$

The continuity of f at the region boundaries is then given by

$$F(x) = f_{\rm I}(u_1, \mu_1) = f_{\rm III}(u_2, \mu_2), \tag{9}$$

where $f_{\rm I}$ and $f_{\rm III}$ are solutions to Eqs. (4) in regions I and III, and where

$$u_j^2 \equiv x^2 + w_j^2\,, \tag{10a}$$

$$\mu_j \equiv w_j / u_j\,, \tag{10b}$$

for $j = 1,2$.

As noted above the inability to match fluxes of order D implied that $G = 0$. We do expect, however, two boundary

conditions to arise from the requirement that the normal flux be continuous, and the condition on G represents only one condition. The other flux condition assures us that the perpendicular (x-directed) flux in region II must account for the difference in the w-directed fluxes at the boundary. To be specific we define velocity flux $\mathbf{S}$ by $\partial f/\partial t + \nabla \cdot \mathbf{S} = 0$, so that upon integrating this equality from w_1 to w_2, we obtain

$$\Delta \frac{\partial F}{\partial t} + \frac{1}{x}\frac{\partial}{\partial x} x \int_{w_1}^{w_2} S_x \, dw + S_w(w_2,x) - S_w(w_1,x) = 0 , \tag{11}$$

where $\Delta \equiv w_2 - w_1$, we have made use of Eq. (8), and also have taken the liberty of writing our fluxes in cylindrical coordinates (w,x).[4]

The x-directed flux in region II arise purely from collisions and may be written, using Eq. (8) as

$$S_x = -\frac{w^2}{u^3}\frac{\partial F}{\partial x} - \frac{\xi x}{u^3}\left(\frac{x\,\partial F/\partial x}{u^2} + F\right). \tag{12}$$

The second term above, which represents energy scatterings, is generally much smaller as $u \to \infty$ than the first term, which arises from pitch angle scattering.

At this point the problem is well-posed as an initial value problem. Given $F(x,t)$ one solves Eq. (4) in regions I and III. Then, using Eq. (11), one may compute $F(x,t+\Delta t)$ and proceed to solve for f in regions I and III at time $t+\Delta t$, given the new boundary condition $f = F(x,t+\Delta t)$. The fluxes S_w are, of course, determined when f is known. This procedure would be very efficient for solving Eq. (4) in the limit $D \to \infty$, since it eliminates the fast time scale $\sim 1/D$. Moreover, by solving for f only where $D(w) = 0$, only the collision terms need be treated. Since the collision terms alone exhibit spherical symmetry, fully implicit numerical methods can then be used. This procedure could be used also in solving Eqs. (1) and (2) with $D \to \infty$, and the approximation in Eq. (12) is good as long as $w_1 \gg 1$. To treat the problem exactly in the limit $D \to \infty$, and be valid also for w_1 small, a more exact expression for S_x must be written, but that presents no particular difficulty.

We should specify now the fluxes S_w to be used in Eq. (11); however, since we are interested only in the steady state of Eq. (11), we can cast it into a slightly different, but more convenient, form by integrating between 0 and some x_0, obtaining

$$-\int_0^{x_0} x\,dx \frac{\partial F}{\partial t} = x_0 \int_{w_1}^{w_2} S_x \, dw + \int_0^{x_0} x\,dx\,[S_w(w_1,x) - S_w(w_2,x)] = 0 , \tag{13}$$

where we took $\partial/\partial t \to 0$ in the steady state. The last term represents the flux of particles into region II for $x < x_0$ from regions I and III. In the steady state, however, this flux must equal the radial flux into regions I and III from the boundary $u = (x_0^2 + w_1^2)^{1/2}$ in region I and $u = (x_0^2 + w_2^2)^{1/2}$ in region III (see Fig. 1). Hence we can rewrite this term as

$$\int_0^{x_0} [S_w(w_1,x) - S_w(w_2,x)]\,x\,dx = -\int_{-1}^{\mu_1} u_1^2 \, S_u(u_1,\mu) d\mu + \int_{\mu_2}^{1} u_2^2 \, S_u(u_2,\mu) d\mu , \tag{14}$$

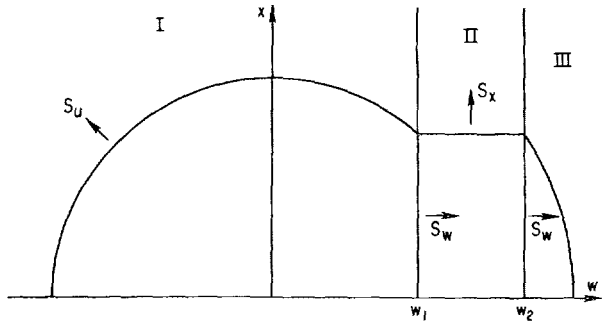

FIG. 1. Balancing the fluxes between regions I, II, and III.

where u_j, μ_j are as defined in Eqs. (10), and

$$u^2 S_u \equiv -\xi\left(\frac{\partial f}{\partial u} + f\right). \tag{15}$$

Thus in the steady state we can write

$$x\int_{w_1}^{w_2} S_x \, dw = -\xi\int_{-1}^{\mu_1}\left(\frac{\partial f}{\partial u} + f\right)_{u=u_1} d\mu + \xi\int_{\mu_2}^{1}\left(\frac{\partial f}{\partial u} + f\right)_{u=u_2} d\mu . \tag{16}$$

We are now in a position to solve for F, using Eqs. (9), (12), and (16), but first we must find f in regions I and III by solving Eq. (4a). This will be done, for $u \to \infty$, in the next section.

III. ASYMPTOTIC STEADY STATE

For the steady state, Eqs. (4) reduce to regions I and III to

$$\frac{\partial}{\partial \mu}(1-\mu^2)\frac{\partial}{\partial \mu} f + \xi u \frac{\partial}{\partial u}\left(\frac{1}{u}\frac{\partial f}{\partial u} + f\right) = 0 . \tag{17}$$

To perform an asymptotic analysis of Eq. (17), we look for solutions exhibiting nearly spherical symmetry. Here we are motivated, in part, by the observation that as $u \to \infty$ the percentage of velocity space covered by the resonant region vanishes as Δ/u. Moreover, there is an expectation that if, in fact, a steady state does exist, the waves should play a smaller and smaller role as $u \to \infty$. Thus we try

$$f = e^{g(u) + h(u,\mu)} , \tag{18a}$$

where

$$g(u) \gg h(u,\mu) , \tag{18b}$$

and

$$\frac{dg}{du} \gg \frac{\partial h}{\partial \mu} . \tag{18c}$$

Plugging Eqs. (18) into Eq. (17), we get

$$-\xi\,[g_{uu} + g_u^2 + (u - 1/u)g_u] \simeq (1-\mu^2)(h_{\mu\mu} + h_\mu^2) - 2\mu h_\mu , \tag{19}$$

where the subscript u or μ indicates derivatives with respect to that variable, and where we have made use of Eq. (18c) in omitting terms proportional to $\partial h/\partial u$. Motivated again by the solution in the absence of waves, where $h = 0$ and $g = -u^2/2$, we look for solutions such that $g_u \gg 1$. From Eq.

(19) we can then expect to also find $h_\mu \gg 1$. Then balancing the nonlinear and highest-order-in-u terms in Eq. (19), we can write

$$(1-\mu^2)\,h_\mu^2 = -\xi\,(ug_u + g_u^2)\,, \tag{20}$$

which we can solve to obtain

$$h = \pm(\theta - \theta_0)k\,, \tag{21a}$$

$$k = \xi^{1/2}|ug_u + g_u^2|^{1/2}\,, \tag{21b}$$

where θ_0 is a constant of integration (that can depend on u, but must be smaller than g) and $1/k$ is treated as an expansion parameter. This expansion is valid so long as

$$k \gg 1, \frac{\partial k}{\partial u}\,. \tag{22}$$

Note also that g is, at this point, an arbitrary function of u. We adopt the notation $g = g_1$ in region I and $g = g_2$ in region III. With a view toward matching to region II, we pick the sign of h in Eq. (21a) such that h is largest at the boundary $w = w_1$ or $w = w_2$, and we pick

$$\theta_0 = \theta_1 \equiv \cos^{-1}\mu_1, \quad \text{in region I}\,, \tag{23a}$$

$$\theta_0 = \theta_2 \equiv \cos^{-1}\mu_2, \quad \text{in region III}\,. \tag{23b}$$

Thus, at the boundary with region II, $h(u,\mu) = 0$. Let

$$F = e^{G(x)}\,, \tag{24}$$

so that to satisfy Eq. (9), we must have

$$G(x) = g_1(u_1) = g_2(u_2)\,, \tag{25}$$

which implies that

$$g_1(u) = G\left[(u^2 - w_1^2)^{1/2}\right], \tag{26a}$$

$$g_2(u) = G\left[(u^2 - w_2^2)^{1/2}\right]. \tag{26b}$$

The solution, then, to Eq. (17), with g_j as in Eq. (26) and G still undetermined, is

$$f = e^{g_1 - k(\theta - \theta_1)}, \quad \text{in region I}\,, \tag{27a}$$

$$f = e^{g_2 + k(\theta - \theta_2)}, \quad \text{in region III}\,. \tag{27b}$$

We now seek to evaluate the right-hand side of Eq. (16). Note that

$$\int_{-1}^{\mu_1}\left(\frac{1}{\mu}\frac{\partial f}{\partial u} + f\right)_{u=u_1} d\mu \simeq \left[\left(\frac{g_{1u}}{u} + 1\right)e^{g_1}\int_{-1}^{\mu_1} e^{-k(\theta-\theta_1)}\,d\mu\right]_{u=u_1}. \tag{28}$$

The integration over μ can be evaluated asymptotically as

$$\begin{aligned}\int_{-1}^{\mu_1} e^{-k(\theta-\theta_1)}\,d\mu &= \int_{\theta}^{\pi} e^{-k(\theta-\theta_1)}\sin\theta\,d\theta \\ &= \int_0^{\pi-\theta_1} e^{-k\chi}(\cos\chi\sin\theta_1 + \sin\chi\cos\theta_1)d\chi \\ &\simeq \frac{(1-\mu_1^2)^{1/2}}{k} + O\left(\frac{1}{k^2}\right) = \frac{x}{ku_1} + O\left(\frac{1}{k^2}\right),\end{aligned} \tag{29a}$$

where k is understood to be $k(u_1)$ and where, in writing the approximate equality, we made use of the fact that $k \gg 1$, but $\pi - \theta_1 \sim O(1)$. Similarly, we find

$$\int_{\mu_2}^{1} e^{k(\theta-\theta_2)}\,d\mu = \frac{x}{k(u_2)u_2} + O\left(\frac{1}{k^2}\right). \tag{29b}$$

Define

$$\begin{aligned}y(x) &\equiv -\frac{1}{x}\frac{dG}{dx} = -\left(\frac{1}{u}\frac{dg_1}{du}\right)_{u=u_1} \\ &= -\left(\frac{1}{u}\frac{dg_2}{du}\right)_{u=u_2},\end{aligned} \tag{30}$$

so that we an write

$$k(u_j) = \xi^{1/2}u_j|y^2 - y|^{1/2}\,, \quad j = 1,2\,. \tag{31}$$

Using Eqs. (24)–(31) in Eq. (16), we can write the right-hand side of Eq. (16) as

$$\text{rhs}(16) = -\left(\frac{\xi(1-y)}{y}\right)^{1/2}\left(\frac{1}{u_1^2} + \frac{1}{u_2^2}\right)xF\,. \tag{32}$$

The left-hand side of Eq. (16) may be written, using Eq. (12), as

$$\text{lhs}(16) = [-(px + \xi x^3 q)y + \xi x r]xF\,, \tag{33}$$

where

$$p(x) \equiv \int_{w_1}^{w_2}\frac{w^2}{u^3}\,dx\,, \tag{34a}$$

$$q(x) \equiv \int_{w_1}^{w_2}\frac{dw}{u^5}\,, \tag{34b}$$

$$r(x) \equiv \int_{w_1}^{w_2}\frac{dw}{u^3}\,. \tag{34c}$$

Equating Eqs. (32) and (33), we obtain

$$-(p + \xi x^2 q)y + \xi r = -\left(\frac{1-y}{y}\right)^{1/2}\frac{\xi^{1/2}}{x}\left(\frac{1}{u_1^2} + \frac{1}{u_2^2}\right), \tag{35}$$

which allows us to determine y. Note that, by inspection of Eq. (35), it is apparent that real solutions y exist only in the interval

$$1 > y > \xi r/(p + \xi x^2 q) > 0\,. \tag{36}$$

The upper limit on y represents a Maxwellian distribution, as can be seen from Eq. (30), i.e., $G = -x^2/2$. Note that this obtains when $w_2 = w_1$, which implies $p = q = r = 0$, and we recover the no-rf case. What Eq. (36) states is that F is a monotonically decreasing function of x, dropping off no faster than a Maxwellian with the bulk temperature. Moreover, note that y is asymptotically bounded below by a nonzero constant for $w_2 \neq w_1$, namely,

$$y > \frac{\xi r}{p + \xi x^2 q} \underset{x\to\infty}{\to} \frac{\xi\Delta}{(w_2^3 - w_1^3)/3 + \xi\Delta}\,, \tag{37}$$

where $\Delta \equiv w_2 - w_1$ is the spectrum width. The implication is that asymptotically F decreases monotonically no slower than a Maxwellian with some temperature greater than the bulk temperature. Such a distribution is eminently normalizable, which shows that a steady state must exist. Finally, note that asymptotically bounding y between constants in Eq. (36), implies by Eq. (31), that as $x \to \infty$, $k \sim x$, which validates our solving Eq. (17) via an expansion in $1/k$.

We now calculate the asymptotic behavior. For $x \to \infty$, we obtain to leading order

$$-\left(\frac{(w_2^3 - w_1^3)}{3} + \xi\Delta\right)y + \xi\Delta = \xi^{1/2}\left(\frac{1-y}{y}\right)^{1/2}. \quad (38)$$

This is a cubic equation for y with one real root on the interval (0,1). Thus y always approaches some constant, which means that F is asymptotically Maxwellian, but at a hotter temperature than the bulk temperature. In effect, the value of y^{-1} is the tail temperature. For most heating or current-drive problems, the case of interest is $w_2^3 - w_1^3 \gg 1, \xi\Delta$. Setting $R \equiv (w_2^3 - w_1^3)/3\xi^{1/2} + \xi^{1/2}\Delta \gg 1$, we have

$$R^2 y^3 + 2\xi^{1/2}\Delta R y^2 + \xi\Delta^2 y = 1 - y. \quad (39)$$

Let $\epsilon = 1/R^{1/3}$ and $y = \epsilon^2 z$; then Eq. (39) becomes

$$z^3 + \epsilon 2\xi^{1/2}\Delta z + \epsilon^2\xi\Delta^2 z = 1 - \epsilon^2 z, \quad (40)$$

and expanding $z = z_0 + \epsilon z_1 + \cdots$, we find

$$z = 1 + \tfrac{2}{3}\xi^{1/2}\Delta\epsilon + \cdots, \quad (41)$$

or

$$y \simeq [(w_2^3 - w_1^3)/3\xi^{1/2}]^{-2/3} + \cdots. \quad (42)$$

For example, if $\xi = 1$, $w_2 = 5$, $w_1 = 3$, the effective temperature as $x \to \infty$ is approximately 10 times the bulk temperature.

At this juncture several caveats ought to be mentioned. The asymptotic analysis indicates that the leading behavior of the tail of the electron distribution function is Maxwellian with a temperature hotter than the bulk temperature. This result implies that f is normalizable and hence tends to a steady state. This is useful to know for aesthetic or numerical purposes. However, the asymptotic result may be valid only at extremely high values of u. At that point the particle dynamics may be affected by phenomena not contained in Eq. (1), such as relativistic effects and radiation, or the model used for the waves in Eq. (2) may no longer be useful. Moreover, even if we do accept Eqs. (1) and (2) as a valid description, the asymptotic result may be valid only at uninterestingly high values of x. On the other hand, as discussed above, the procedure outlined here is of more general utility than in merely calculating the asymptotic temperature.

IV. CONNECTING TO THE BULK DISTRIBUTION

The asymptotic methods of Sec. III are not readily extendable to describing f, with rigor, over all velocity space. Nonetheless some progress can be made. Here we shall content ourselves with writing an analytic expression for f that is asymptotically correct as $u \to \infty$ and as $u \to 0$, and is a reasonable approximation between these limits.

Our approach is as follows: suppose that the asymptotic solution holds for $x > x_B$, where x_B is to be determined later. Then by Eq. (35) we can determine $y(x)$, which, in turn, by Eqs. (24) and (30) gives us $F(x)$ in the region $x > x_B$. Finally, we can use Eqs. (26) and (27) to find f in the disjoint regions I ($w < w_1, u > u_{B1}$) and III ($w > w_2, u > u_{B2}$), where $u_{Bj}^2 \equiv x_B^2 + w_j^2$, $j = 1, 2$ (see Fig. 2). This determines f up to a multiplicative constant in the resonant region $x > x_B$ and in the disjoint nonresonant regions I and III. In principle we can use this solution to specify f up to a multiplicative constant on the finite common boundary of these regions, which serves as proper boundary condition for solving the Fokker–Planck equation in the complement space (i.e., $x < x_B$ in the resonant region, etc.). The solution is specified up to a constant which can be found via a normalization condition on f.

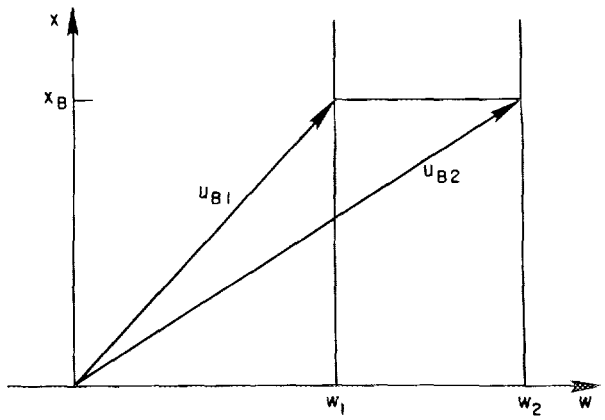

FIG. 2. Definitions of x_B, u_{B1}, and u_{B2}. Note that $\mu_{B1} \equiv w_1/u_{B1}$ and $\mu_{B2} \equiv w_2/u_{B2}$.

It may appear curious that a fully specified problem was obtained by matching only f at a boundary, rather than both f and its normal derivative. Here, however, the solution in one region is valid asymptotically and hence, by construction, insensitive to the details of the solution in the complement space. In fact, specifying either f or its normal derivative should give the same solution in the complement space for x_B sufficiently large.

It remains, however, to solve the Fokker–Planck equation in the complement space. Although it is easy to write an analytic solution in the limit $u \to 0$, the region $u \sim w_1$ will be difficult to treat with rigor. Our approach will be to fit the $u \to 0$ solution to the asymptotic solution notwithstanding, but subject to constraints on matching the fluxes at $w = w_1, w_2$ with $x < x_B$. The boundary $x = x_B$, at which the matching to the asymptotic solution takes place and which is so far a free parameter, will be chosen so that the fit is optimized. Although a solution thus obtained is not correct everywhere in any rigorous asymptotic sense, it should be adequate for many purposes.

Accordingly, we write the solution to Eq. (17) as $u \to 0$ by exploiting the vanishing of the angular dependence in the highly collisional subthermal regime. Such a solution may be constructed formally by solving the equation

$$\xi u \frac{\partial}{\partial u}\left(\frac{1}{u}\frac{\partial f}{\partial u} + f\right) = -\delta\frac{\partial}{\partial\mu}(1-\mu^2)\frac{\partial}{\partial\mu}f, \quad (43)$$

where f is to be formally expanded as $f = f_0 + \delta f_1 + \cdots$, with δ a formal expansion parameter that is treated as small when expanding but later equated to unity. Equation (43) treats the region $w < w_1$, $u < u_{B1}$. To zeroth order, we find

$$f_0 = A(\mu) + B(\mu)\exp(-u^2/2), \quad (44)$$

where A and B are constants to be determined by boundary conditions. Assume that $F(x)$ is known not only for $x > x_B$, but for $x < x_B$ as well. Then, requiring that as $u \to 0$, $f \to f_N e^{-u^2/2}$, where f_N is a constant to be found by normalizing, matching f to the asymptotic solution at $u = u_{B1}$, and matching f to the solution in the resonant region at $w = w_1$, we obtain

$$f=f_B(\mu)+\left(\frac{f_N-f_B(\mu)}{1-\exp(-u_{B1}^2/2)}\right)\times\left[\exp\left(\frac{-u^2}{2}\right)-\exp\left(\frac{-u_{B1}^2}{2}\right)\right],\quad \mu<\mu_{B1} \tag{45a}$$

and

$$f=F\left(\frac{(1-\mu^2)^{1/2}w_1}{\mu}\right)+\left(\frac{f_N-F}{1-\exp(-w_1^2/2\mu^2)}\right)\times\left[\exp\left(\frac{-u^2}{2}\right)-\exp\left(-\frac{w_1^2}{2\mu^2}\right)\right],\quad \mu>\mu_{B1}\,, \tag{45b}$$

where $f_B(\mu)$ is the given boundary condition at $u=u_{B1}$, $F(x)$ is the assumed solution in the resonant region $x<x_B$ (which we have yet to find), and $\mu_{Bj}\equiv w_j/u_{Bj}$, $j=1,2$.

To find $F(x)$ for $x<x_B$, we substitute Eq. (45) into Eq. (16), and, assuming $u_{B1}\gg 1$, we obtain

$$-x\int_{w_1}^{w_2}S_x\,dw\simeq+\xi(1+\mu_{B1})\times\left[\bar{f}_B-f_N\exp\left(\frac{-u_{B1}^2}{2}\right)\right]+w_1\int_x^{x_B}\frac{x}{(x^2+w_1^2)^{3/2}}\times\left[F(x)-f_N\exp\left(-\frac{w_1^2}{2}-\frac{x^2}{2}\right)\right]dx\,, \tag{46}$$

where we defined

$$(1+\mu_{B1})\bar{f}_B\equiv\int_{-1}^{\mu_{B1}}f_B(\mu)d\mu\,, \tag{47}$$

and ignored contributions from the boundary at $w=w_2$. Satisfying Eq. (46) at $x=0$ gives us the condition

$$w_1\int_0^{x_B}\frac{x}{(x^2+w_1^2)^{3/2}}\left[F(x)-f_N\exp\left(-\frac{w_1^2}{2}-\frac{x^2}{2}\right)\right]dx=-\xi(1+\mu_{B1})(\bar{f}_B-f_N\,e^{-u_{B1}^2/2})\,. \tag{48}$$

Several notable features of allowed solutions are exhibited by Eq. (48). Note that, under rf excitation, we expect f to be flattened for $u>w_1$, such that a superthermal electron tail is formed with $f_B>f_N\exp(-u_{B1}^2/2)$. This implies, however, that the right-hand side (48) is negative, which requires that $F(x)<f_N\exp(-w_1^2/2-x^2/2)$ for at least some $x<x_B$. Since the opposite inequality is satisfied for $x\sim x_B$, and F is expected to fall off more slowly than a Maxwellian with the bulk temperature, it follows that $F(0)\gg f_N\exp(-w_1^2/2)\equiv a$, where a can be thought of as the value of $f(w=w_1,x=0)$ in the absence of rf. This gives us the interesting result, already seen in numerical calculations, that in the resonant region near $x=0$, the rf excitation actually depletes electrons. Note that for $f_B=f_N\exp(-u_{B1}^2/2)$, we see that $F(x)=a\exp(-x^2/2)$ solves Eq. (48), thus giving the unperturbed Maxwellian solution of the no-rf case.

Plugging Eq. (48) into Eq. (46) and taking the limit $x\ll w_1$ allows us to write

$$\epsilon\int_0^x x\left[F(x)-a\exp\left(\frac{-x^2}{2}\right)\right]dx=-x\int_{w_1}^{w_2}S_x\,dw\simeq xp\frac{dF}{dx}+\epsilon x^2F\left(1-\frac{w_1^2}{w_2^2}\right), \tag{49}$$

where $\epsilon=\xi/w_1^2\ln(w_2/w_1)$, and the last approximate equality evaluated S_x from Eq. (12), taking the limit $x\to 0$. Here $p\to\ln(w_2/w_1)$. From Eq. (49) it can be seen that in the presence of rf excitation, i.e., $p\neq 0$, $xF_x\sim O(\epsilon)$. Moreover, $F(0)\ll a$ implies $xF_x<0$ near $x=0$, and by Eq. (48) we see that the left-hand side of Eq. (49) is negative also at $x=x_B$ giving $xF_x<0$ there, too. Together, the implication is that F is a monotonically decreasing function of x in the region $0<x<x_B$.

We can solve Eq. (49) most easily by successive iterations, given ϵ small. An approximate solution is obtained by setting $F=F_0\exp[\epsilon g(x)]$, and for ϵg small, i.e., x not too large, we obtain

$$g=\frac{1}{p}\int_0^x\left[xF_0\left(\frac{w_1^2}{w_2^2}-\frac{1}{2}\right)+a\frac{\exp(-x^2/2)-1}{x}\right]dx\,. \tag{50}$$

Note that near $x=0$, F exhibits Maxwellian behavior with an effective temperature of $\epsilon(a/2+F_0/2-F_0w_1^2/w_2^2)$. Note, too, that consistent with numerical solutions (to be shown in the next section) the temperature near $x=0$ increases with x.

We now match Eq. (50) onto the asymptotic solution. Matching f gives us

$$F_B=F_0\,e^{-\epsilon g(x_B)}\,. \tag{51}$$

Matching dF/dx gives us

$$\frac{-x_B}{1+\xi x_B^2/\epsilon^2}F_B=\frac{\epsilon}{p}\left\{xF_0\left(\frac{w_1^2}{w_2^2}-\frac{1}{2}\right)+\frac{a}{x}\left[\exp\left(\frac{-x_B^2}{2}\right)-1\right]\right\}F_B\,. \tag{52}$$

Finally, satisfying Eq. (48) gives

$$\frac{1}{w_1^2}\int_0^{x_B}x\left[F-a\exp\left(\frac{-x^2}{2}\right)\right]dx=\xi(1+\mu_{B1})[\bar{f}_B-a\exp(-x_B^2/2)]\,. \tag{53}$$

Equations (51)–(53) represent three equations with which we find the unknowns F_0, x_B, and F_B.

An approximate solution to Eqs. (51)–(53) is given by

$$F(x)=F_0\exp[-(a/F_0-1)\epsilon x^2/4],\quad x<x_B\,, \tag{54}$$

where x_B solves

$$\exp(x_B^2/2)-1=2y_B/\epsilon\,, \tag{55}$$

$y_B=y(x_B)$ may be solved for from Eq. (55), and

$$F_0=a\exp(-x_B^2/2)=f_N\exp[-(w_1^2+x_B^2)/2]\,. \tag{56}$$

The solution for $x>x_B$ is given by

$$F=F_B\exp\left(-\int_{x_B}^x xy\,dx\right), \tag{57}$$

with y determined from Eq. (55) and

$$F_B=F_0\exp[-\epsilon(a/F_0-1)x_B^2/4]\,. \tag{58}$$

Using Eqs. (54)–(56) and Eq. (45), we can now solve for f when $w<w_1$. (In the small and nonconsequential region $\mu>\mu_{B2}$ and $u^2<x_B^2+w_2^2$, we assume f is independent of μ for plotting purposes only.) From Eqs. (57) and (58) we now

have the multiplicative constant we sought for the asymptotic region. This extended solution is admittedly rough and nonrigorous, but it may be adequate for many purposes. Exactly how well it approximates numerically derived solutions will be discussed in the next section.

V. COMPARISON WITH THE NUMERICAL SOLUTIONS

As a check to the analytical solutions, we numerically integrated the Fokker–Planck equation until a steady state was reached. The electron distribution function so obtained may be compared with the analytical solution.

The numerical code is the same as employed in an earlier paper, Ref. 4, which solved the Fokker–Planck equation [written here as Eqs. (1), (2), and (3c)] in spherical coordinates with a boundary condition that $\mathbf{S}\cdot\hat{u} = 0$ at $u = u_{\max}$. Collisions are treated assuming that the ion and electron backgrounds are stationary Maxwellians. In order to accelerate the approach to steady state, the Fokker–Planck equation is recast as

$$\frac{\partial f}{\partial t} + h(u)\nabla\cdot\mathbf{S} = 0\,, \tag{59}$$

where $h(u)$ is some positive function. Obviously that equation has the same steady state as where $h(u) = 1$, namely $\nabla\cdot\mathbf{S} = 0$. However, by choosing $h(u)$ to be some increasing function of u we can accelerate the normally slow relaxation of the fast electrons. Here we choose $h(u) = 1 + u$. In addition, we replace the quasilinear diffusion coefficient $D(w)$ by $D(w)/h(u)$. This avoids the numerical problems associated with large diffusion coefficients but does not affect the solution as long as D_0 is sufficiently large. In all the examples shown here, $D_0 = 10$.

As a typical case, we consider $w_1 = 5$, $w_2 = 8$, $Z_i = 1$. Figure 3 shows contour plots of the analytic and numerical steady-state distributions. The contour levels are chosen in order to give equally spaced contours for a Maxwellian. The analytic function correctly predicts the qualitative features of the numerical solution, namely, the Maxwellian nature of f for $u < w_1$, the parallel flattening in the plateau, the increased perpendicular temperature in the plateau, and the increased perpendicular and parallel temperatures in the nonresonant region for $u > w_1$. There are two aspects of the solution where there is disagreement: the contours for the analytic f in the nonresonant regions (I and III) cut in too quickly. This is because the form of f in the nonresonant region is only correct asymptotically. In particular, $\partial f/\partial\mu$ has a weak (square root) singularity at $\mu = \pm 1$. Note, however, that better agreement is obtained at $\mu = \pm 1$ for larger u, where the asymptotic solution is expected to be better.

One may wonder why the solution elsewhere is so good. The reason is that the problems near $\mu = \pm 1$ only affect the form of f elsewhere through their contribution to the flux. However, the flux is multiplied by $(1-\mu^2)^{1/2}$, which is small.

The other disagreement is the temperature for $u \approx u_{\max}$. The numerical solution shows a significantly lower temperature. However, this is just an artifact of the no-flux boundary condition at u_{max} for the numerical solution, as can be checked by carrying out the integrations in a larger domain.

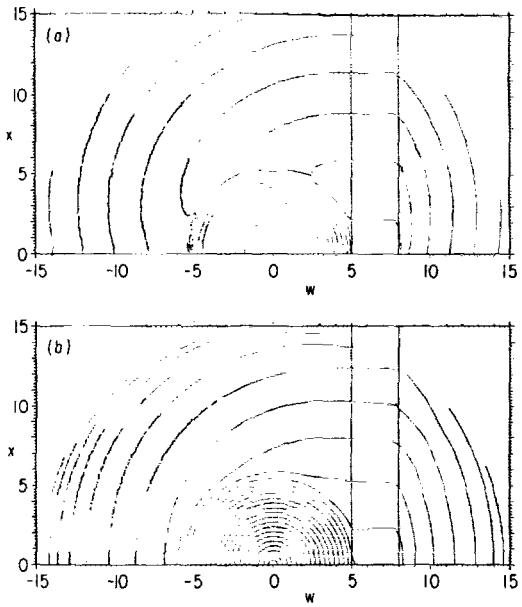

FIG. 3. Contour plots of the analytic (a) and numerical (b) steady-state distribution functions for $w_1 = 5$, $w_2 = 8$, and $Z_i = 1$.

Turning now to a more quantitative comparison between the two solutions, we plot in Fig. 4, the perpendicular distribution function in the resonant region $f[(w_1 + w_2)/2, x] = F(x)$. The whole analytic solution for $u > w_1$ hangs on the form of this function, and it is therefore a sensitive test of the soundness of the analytic method. In this figure there are two points worthy of note. First, the slope of $F(x)$ is accurately given by the analytic solution. This is further checked in Fig. 5, where we plot $T_\perp(x)$, and local perpendicular temperature has been defined by $F(x) = \exp\{-\int[x/T_\perp(x)]dx\}$. At high x the two temperatures differ by about 20%, which is good agreement considering that the analytic result should only hold asymptotically. It is also remarkable how well the analytic form for $T_\perp(x)$ agrees with the numerical result when x is small. Incidentally, the ripples in the numerical result for $T_\perp(x)$ are again an artifact of the numerics. These arise because the resonant region is not lined up with the numerical grid. The effect is magnified because it is necessary to perform a numerical differentiation to obtain $T_\perp(x)$. The final dip in the numerical

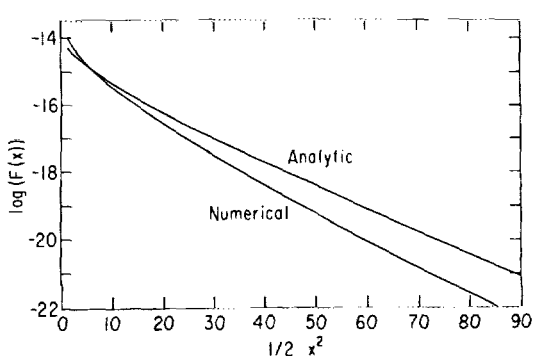

FIG. 4. The perpendicular distribution function $F(x)$ for the case shown in Fig. 3.

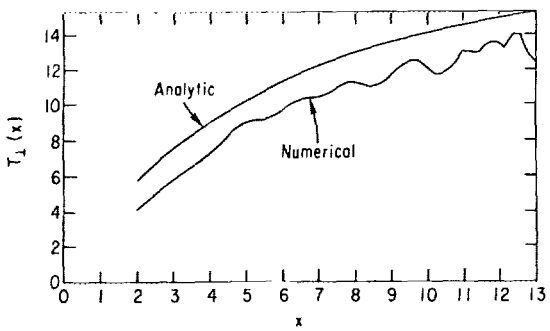

FIG. 5. The perpendicular temperature $T_\perp(x)$ for the case shown in Fig. 3.

$T_\perp(x)$ is because of the boundary, on which we had imposed a no-flux condition.

The second point about Fig. 4 is the comparison of the results for $F(0)$. Let us recall that the one-dimensional theory[3] has $F(0) = \exp(-w_1^2/2)$ for $w_1 \gg 1$. [Here and in Fig. 5 we have divided out the normalizing constant $(2\pi)^{-3/2}$.] The two-dimensional result also has this for its leading behavior. Now we cannot numerically specify w_1 to closer than Δu, the grid spacing. That means we expect a numerical error in $\log[F(0)]$ on the order of $w_1 \Delta u \simeq 1$ (for $w_1 = 5$ and $\Delta u = 0.2$). Given this, the agreement between the numerical and analytical values of $\log[F(0)]$ is extremely good since they differ by only 0.3. Note too that $\log[F(0)]$ is less than its one-dimensional value of $-w_1^2/2 = 12.5$ by about 1.5. This means that the starting height of the plateau is below the one-dimensional value by a factor of 4.5. (This effect, which was observed in the early numerical solutions, was the motivation behind the separate analysis in the region $w < w_1$, $x \simeq 0$.)

In order to complement these results, we give $F(x)$ for three other cases in Fig. 6. These show that the analytical solution works well for both narrow and broad spectra and for a range of Z_i. We note, however, that the numerical results consistently give lower results of the perpendicular temperature at large x. This, however, is the regime where we trust the analytical solution (which becomes increasingly accurate for $x \to \infty$) more than the numerical solution. There are two possible problems with the numerical solution. First, it may take an extremely long time for the steady state to be reached. The other potential problem with the numerical solution is that small errors in computing the flux S may alter the steady state solution appreciably. These errors may arise either from not taking $D_0 = \infty$, or from computing S by numerically differencing f. The numerical code therefore solves

$$\nabla\cdot[\mathbf{S}(f+\delta f) + \delta\mathbf{S}(f+\delta f)] = 0\,,$$

instead of

$$\nabla\cdot\mathbf{S}(f) = 0\,.$$

In cases where the magntitude of S varies over orders of magnitude, the relative error $\delta f/f$ may be large in some regions (particularly where f is small) even when the relative error in S, $\delta S/S$, is small everywhere.

The problems with the numerical solutions only affect the higher energy distribution. The low-order moments such

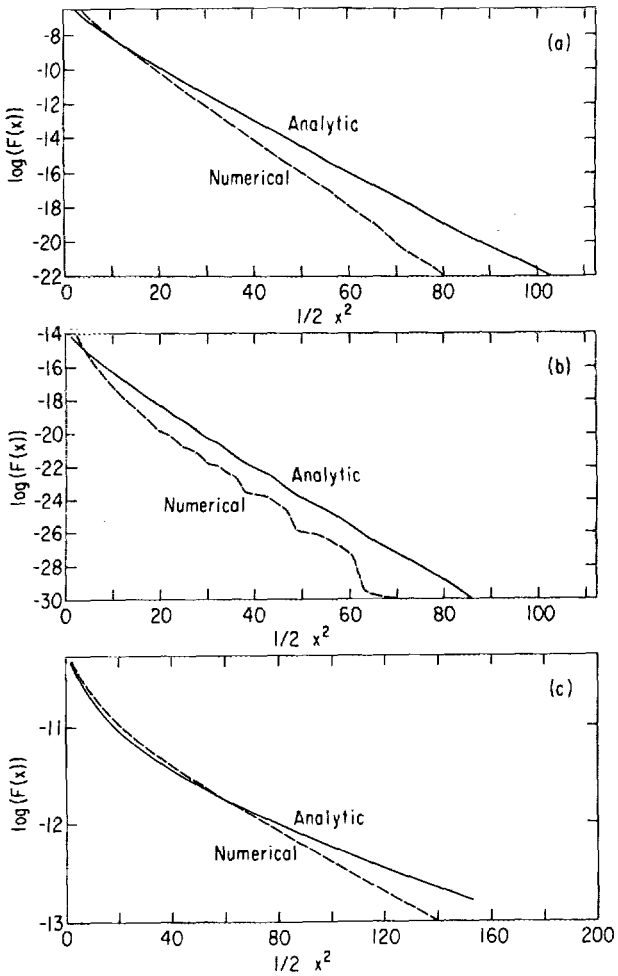

FIG. 6. The perpendicular distribution function $F(x)$ for (a) $w_1 = 3$, $w_2 = 5$, $Z_i = 1$; (b) $w_1 = 5$, $w_2 = 6$, $Z_i = 1$; (c) $w_1 = 4$, $w_2 = 15$, $Z_i = 4.5$.

as the current and power dissipated are accurately given by the numerical solution and furnish another check to the analytical solution. This comparison is made in Table I. The figures for the current differ by at most a factor of 2, which constitutes good agreement given the difficulty in defining w_1 numerically. The efficiency J/P_d is easier to measure numerically and, except for the case of a wide spectrum, the agreement is better ($\sim 30\%$). The error here probably arises from the contribution to P_d from the low-x part of the resonant spectrum, which is treated less exactly. This region is larger when the spectrum is wide, leading to the bigger error. The method of defining the power dissipated in the analytical solution deserves comment. Since this solution is only an approximate steady state, there is no unique definition of P_d.

TABLE I. Comparison of J and J/P_d.

w_1	w_2	Z_i	J_{num}	J_{analy}	$(J/P_d)_{num}$	$(J/P_d)_{analy}$
5	8	1	6.0×10^{-5}	7.0×10^{-5}	35.7	45.0
3	5	1	6.6×10^{-2}	5.1×10^{-2}	14.8	17.6
3	6	1	1.1×10^{-5}	1.5×10^{-5}	28.9	36.9
4	15	4.5	4.9×10^{-2}	5.0×10^{-2}	49.1	142

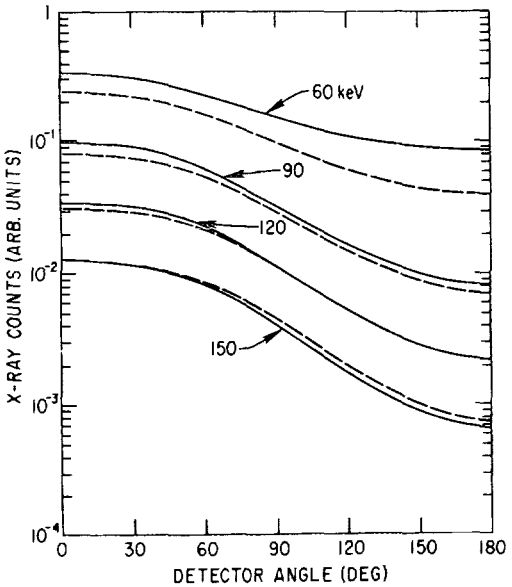

FIG. 7. Comparison of the bremsstrahlung emission from the numerical (solid lines) and analytic (dashed lines) electron distribution functions for the case shown in Fig. 3. A background temperature of 5 keV is assumed.

For instance, the collisional power transferred to the bulk need not balance the rf power absorbed. Here we define the power absorbed in terms of the fluxes in the resonant region, since it is here that the analytical solution is most reliable. The rf power absorbed by the plasma is

$$P_d = \int_{w_1}^{w_2} dw \int_0^\infty x\,dx\,\mathbf{u}\cdot\mathbf{S}^{(\mathrm{rf})}, \tag{60}$$

where $\mathbf{S}^{(\mathrm{rf})}$ is the rf-induced flux. In our case $\mathbf{S}^{(\mathrm{rf})} = \hat{w} S_w^{(\mathrm{rf})}$, where $S_w^{(\mathrm{rf})} = -D_0\,\partial f/\partial w$. This quantity is not directly known, since in the analysis we took $D_0 \to \infty$, $\partial f/\partial w \to 0$, so we relate it to the collisional flux by

$$S_w^{(\mathrm{rf})} = S_w - S_w^{(c)}, \tag{61}$$

where S_w is the total w-directed flux. Substituting this into the expression for P_d gives two terms. The first involves the integral

$$\int_0^\infty x\,dx\,S_w,$$

which vanishes in the steady state (the total flux through an infinite plane is zero). The remaining term gives

$$P_d = -\int_{w_1}^{w_2} dw \int_0^\infty x\,dx\,w S_w^{(c)}. \tag{62}$$

In the resonant region, $f(x,w) = F(x)$ and so

$$-S_w^{(c)} = \frac{\xi w}{u^3}\left(\frac{x}{u^2}\frac{d}{dx} + 1\right)F - \frac{xw}{u^3}\frac{dF}{dx}. \tag{63}$$

The w integrals can be performed analytically, i.e.,

$$\int \frac{w^2}{u^3}\,dw = \log\left(\frac{w+u}{x}\right) - \frac{w}{u}, \tag{64}$$

and

$$\int \frac{w^2}{u^5}\,dw = \frac{1}{3}\frac{w^3}{x^2u^3}. \tag{65}$$

Thus P_d is given by a one-dimensional integral involving $F(x)$.

There is one final check of the analytical solution and that is the bremsstrahlung emissions. These are compared for the case $w_1 = 5$, $w_2 = 8$ in Fig. 7. Here we assumed that the plasma temperature was $T_e = 5$ keV and we have only included the contributions from electrons with speeds up to $u = 15$. Given the agreement in f, it is not surprising that we see a close fit here also. Since the bremsstrahlung is mainly emitted by the fast electrons, the defects of two analytical solutions near $u = w_1$ do not show up here. When comparing the other cases we see differences in the intensities of the high-energy emissions. This is because of the lower temperature given by the numerical solution. However, as discussed above, the analytical solution is more trustworthy here.

VI. CONCLUSIONS

We have developed an asymptotic solution for the Fokker–Planck equation in the presence of strong rf. This shows that a steady state is achieved; there is no rf runaway even when $D_0 \to \infty$. Although the solution is asymptotic, it gives a good fit to the numerial solutions even for low x; and by matching the asymptotic solution to an interior solution, we can derive an approximate solution for f for all $\mathbf{u}$.

This may be used for a number of purposes: the bremsstrahlung may be estimated from the analytical solution and this may be used to reduce the experimental bremsstrahlung data to a few important experimental parameters, namely w_1, w_2, and Z_i. In practice the bremsstrahlung emission may be affected by relativistic corrections to the collision operator and other phenomena, such as synchrotron radiation, which principally affect the high-energy electrons. The analytic method given in this paper could probably be extended to include such effects.

The other important area where knowledge of the distribution function is useful is in determining transport coefficients. The transport of electron energy depends on the perpendicular distribution of electrons. Also the success of rf current ramp-up experiments depends on the resistivity of the electrons to the induced back current. This resistivity depends on f.

Finally, knowledge of the asymptotic distribution has highlighted the difficulty of computing the high-energy distribution by conventional means and has suggested a way in which the numerical solution may be improved to deal with the strong-rf limit, as discussed above [following Eq. (12)].

ACKNOWLEDGMENTS

We would like to thank J. E. Stevens for making his bremsstrahlung program available to us.

This work was supported by the U. S. Department of Energy Contract No. DE-ACO2-76-CHO-3073.

[1] B. A. Trubnikov, in *Reviews of Plasma Physics*, edited by M. A. Leontovich (Consultants Bureau, New York, 1965), Vol. 1, p. 105.
[2] R. W. Harvey, K. D. Marx, and M. G. McCoy, Nucl. Fusion **21**, 153 (1981).
[3] N. J. Fisch, Phys. Rev. Lett. **41**, 873 (1978).
[4] C. F. F. Karney and N. J. Fisch, Phys. Fluids **22**, 1817 (1979).
[5] N. J. Fisch, Ph.D. thesis, Massachusetts Institute of Technology, 1978.
[6] N. J. Fisch and A. H. Boozer, Phys. Rev. Lett. **45**, 720 (1980).